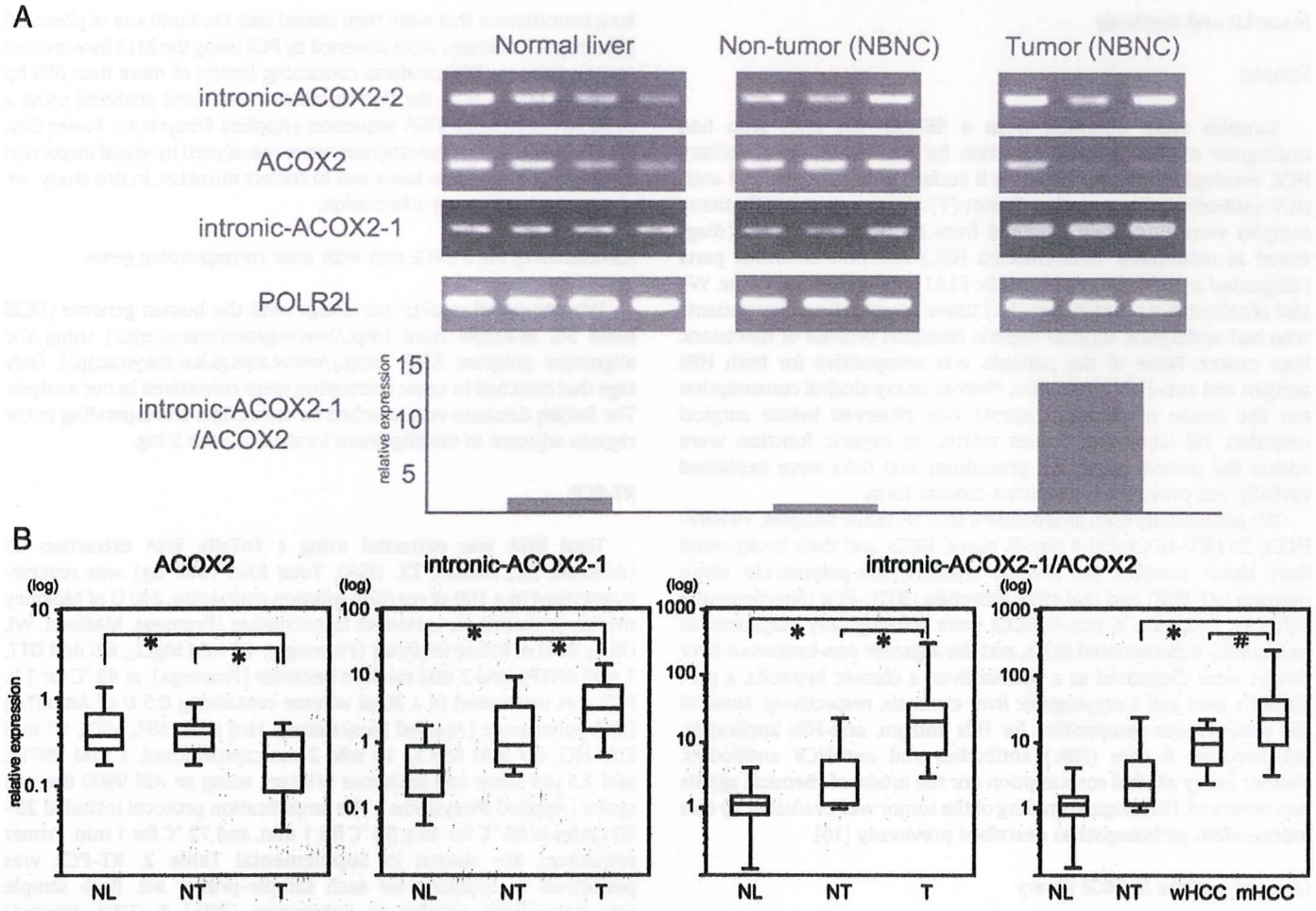

Fig. 1. (A) RT-PCR results of *ACOX2* and *ACOX2* intronic RNAs in independent NL, NT (non-B, non-C), and T (non-B, non-C) samples. RT-PCR was performed in triplicate for each sample-primer set from cDNA. The PCR products were semi-quantitatively analyzed with ImageJ software and calculated as levels relative to *polymerase (RNA) II (DNA directed) polypeptide L* (*POLR2L*). The bar graph indicates the expression ratio of intronic-ACOX2-1 to canonical ACOX2. The expression pattern of intron 1 was different from that of canonical *ACOX2*. (B) RTD-PCR analysis of *ACOX2* and *ACOX2* intronic RNAs in NL, T (HBV-related, HCV-related, and non-B, non-C), and NT tissues. Quantitative RTD-PCR was performed in duplicate for each sample-primer set from cDNA. Each sample was normalized relative to *POLR2L*. All HCC tissues were pathologically diagnosed as well differentiated HCC (wHCC) or moderately differentiated HCC (mHCC). Kruskal–Wallis tests and Mann–Whitney *U* tests were used for statistical analysis. ACOX2, acyl-Coenzyme A oxidase 2; HCC, hepatocellular carcinoma; NL, normal liver; NT, non-tumor; RT-PCR, reverse transcriptase-polymerase chain reaction; RTD-PCR, real-time detection-PCR; T, tumor. $^{*}P<0.01$, $\#P<0.05$.

were able to clone the intron-origin *ACOX2* RNAs (intronic-*ACOX2-1, 2*) for the first time and found that intronic-*ACOX2-1* was significantly overexpressed in T compared with NT and NL. The ratio of intronic-*ACOX2-1* and canonical *ACOX2* (relative intronic-*ACOX2*) was progressively up-regulated from NL via the background liver to HCC. Importantly, the expression of relative intronic-*ACOX2* was more up-regulated in moderately differentiated HCC than in well-differentiated HCC. The intronic difference in expression might be due to a polymorphism, since the 5′SAGE library for NL and T were from different people. The mechanisms of stepwise increase of intronic-*ACOX2* in the process of hepatocarinogenesis should be clarified in future.

ACOX2 is a rate-limiting enzyme of branched-chain acyl-CoA oxidase involved in the degradation of long branched fatty acid and bile acid intermediates in peroxisomes. *ACOX2* expression was associated with the differentiation state of hepatocytes and was repressed under the undifferentiated phase of human hepatoma cell lines [24]. A decreased *ACOX2* expression was also reported in prostate cancer [25]. Here, the expression of canonical *ACOX2* was decreased, while that of intronic-*ACOX2-1* was increased in HCC. The deduced amino acid of intronic-*ACOX2-1* encodes the C-terminal (from 386 to 681 amino acids) of canonical *ACOX2*, lacking the active sites for FAD binding and a fatty acid as the substrate, suggesting that the protein may be functionally departed [26]. The biological role of the increased intronic-*ACOX2-1* was not clear, but it might be reflected by the activation of peroxisome proliferators-activated receptor alpha (PPARA). It is reported that mice lacking ACOX1, another rate-limiting enzyme in peroxisomal straight-chain fatty acid oxidation, developed steatosis and HCC characterized by increased mRNA and protein expression of genes regulated by PPARα [27]. The importance of PPARα activation in HCC development has been recently reported using HCV core protein transgenic mice [28]. Moreover, the overexpression of alpha-methylacyl-CoA racemase (AMACR), an enzyme for branched-chain fatty acid beta-oxidation, is reported to be a reliable diagnostic marker of prostate cancer and is associated with the decreased expression of ACOX2 [25]. Therefore, the expression of intronic-*ACOX2-1* might open the door for further investigations of their potential clinical use, e.g., serving as diagnostic markers of HCC, although the functional relevance of this gene should be further clarified.

In conclusion, we report the first comprehensive transcriptional analysis of non-B, non-C HCC, NT background liver, and NL tissue, based on 5′SAGE. This study offers new insights into the transcriptional changes that occur during HCC development as well as the molecular mechanism of carcinogenesis in the liver. The results suggest the presence of unique intron-origin RNAs that are useful as diagnostic markers and may be used as new therapeutic targets.

Please cite this article as: Y. Hodo, et al., Comprehensive gene expression analysis of 5′-end of mRNA identified novel intronic transcripts associated with hepatocellular carcinoma, Genomics (2010), doi:10.1016/j.ygeno.2010.01.004

Material and methods

Samples

Samples were obtained from a 56-year-old man who had undergone surgical hepatic resection for the treatment of solitary HCC. Serological tests for hepatitis B surface (HBs) antigen and anti-HCV antibodies were negative. Tumor (T) and non-tumor (NT) tissue samples were separately obtained from the tumorous parts (diagnosed as moderately differentiated HCC) and non-tumorous parts (diagnosed as mild chronic hepatitis: F1A1) of the resected tissue. We also obtained five normal liver (NL) tissue samples from five patients who had undergone surgical hepatic resection because of metastatic liver cancer. None of the patients was seropositive for both HBs antigen and anti-HCV antibodies. Neither heavy alcohol consumption nor the intake of chemical agents was observed before surgical resection. All laboratory values related to hepatic function were within the normal range. All procedures and risks were explained verbally and provided in a written consent form.

We additionally used independent four NL tissue samples, 19 HBV-HCCs, 20 HCV-HCCs and 4 non-B, non-C HCCs, and their background liver tissue samples for reverse transcriptase-polymerase chain reaction (RT-PCR) and real-time detection (RTD)-PCR (Supplemental Table 1). Four non-B, non-C HCCs were histologically diagnosed as moderately differentiated HCCs, and the adjacent non-cancerous liver tissues were diagnosed as a normal liver, a chronic hepatitis, a pre-cirrhotic liver and a cryptogenic liver cirrhosis, respectively. None of the patients was seropositive for HBs antigen, anti-HBs antibodies, anti-hepatitis B core (HBc) antibodies and anti-HCV antibodies. Neither heavy alcohol consumption nor the intake of chemical agents was observed. Histological grading of the tumor was evaluated by two independent pathologists as described previously [16].

Generation of the 5′ SAGE library

5′SAGE libraries were generated as previously described [14]. Five to ten micrograms of poly(A)+RNA was treated with bacterial alkaline phosphatase (BAP; TaKaRa, Otsu, Japan). Poly(A)+RNA was extracted twice with phenol: chloroform (1:1), ethanol precipitated, and then treated with tobacco acid pyrophosphatase (TAP). Two to four micrograms of the BAP-TAP-treated poly(A)+RNA was divided into two aliquots and an RNA linker containing recognition sites for *Eco*RI/*Mme*I was ligated using RNA ligase (TaKaRa): one aliquot was ligated to a 5′-oligo 1 (5′-GGA UUU GCU GGU GCA GUA CAA CGA AUU CCG AC-3′) linker, and the other aliquot was ligated to a 5′-oligo 2 (5′-CUG CUC GAA UGC AAG CUU CUG AAU UCC GAC-3′) linker. After removing unligated 5′-oligo, cDNA was synthesized using RNaseH-free reverse-transcriptase (Superscript II, Invitrogen, Carlsbad, CA, USA) at 12 °C for 1 h and 42 °C for the next hour, using 10 pmol of dT adapter-primer (5′-GCG GCT GAA GAC GGC CTA TGT GGC CTT TTT TTT TTT TTT TTT-3′). After first-strand synthesis, RNA was degraded in 15 mM NaOH at 65 °C for 1 h. cDNA was amplified in a volume of 100 μl by PCR with 16 pmol of 5′ (5′ [biotin]-GGA TTT GCT GGT GCA GTA CAA-3′ or 5′[biotin]-CTG CTC GAA TGC AAG CTT CTG-3′) and 3′ (5′-GCG GCT GAA GAC GGC CTA TGT-3′) PCR primers. cDNA was amplified using 10 cycles at 94 °C for 1 min, 58 °C for 1 min, and 72 °C for 2 min. PCR products were digested with the *Mme*I type IIS restriction endonuclease (NEB, Pickering, Ontario, Canada). The digested 5′-terminal cDNA fragments were bound to streptavidin-coated magnetic beads (Dynal, Oslo, Norway). cDNA fragments that bound to the beads were directly ligated together in a reaction mixture containing T4 DNA ligase in a supplied buffer for 2.5 h at 16 °C. The ditags were amplified by PCR using the following primers: 5′ GGA TTT GCT GGT GCA GTA CA 3′ and 5′ CTG CTC GAA TGC AAG CTT CT 3′. The PCR products were analyzed by polyacrylamide gel electrophoresis (PAGE) and digested with *Eco*RI. The region of the gel containing the ditags was excised and the fragments were self-ligated to produce long concatamers that were then cloned into the *Eco*RI site of pZero 1.0 (Invitrogen). Colonies were screened by PCR using the M13 forward and reverse primers. PCR products containing inserts of more than 600 bp were sequenced with Big Dye terminator ver.3 and analyzed using a 3730 ABI automated DNA sequencer (Applied Biosystems, Foster City, CA, USA). All electrophoretograms were reanalyzed by visual inspection to check for ambiguous bases and to correct misreads. In this study, we obtained 19–20 bp tag information.

Association of the 5′SAGE tags with their corresponding genes

We attempted to align our 5′tags with the human genome (NCBI build 36, available from http://www.genome.ucsc.edu/) using the alignment program ALPS (http://www.alps.gi.k.u-tokyo.ac.jp/). Only tags that matched in sense orientation were considered in our analysis. The RefSeq database was searched for transcripts corresponding to the regions adjacent to the alignment location of each 5′tag.

RT-PCR

Total RNA was extracted using a ToTally RNA extraction kit (Ambion, Inc., Austin, TX, USA). Total RNA (500 ng) was reverse-transcribed in a 100-μl reaction solution containing 240 U of Moloney murine leukemia virus reverse transcriptase (Promega, Madison, WI, USA), 80 U of RNase inhibitor (Promega), 4.6 mM $MgCl_2$, 6.6 mM DTT, 1 mM dNTPs, and 2 mM random hexamer (Promega), at 42 °C for 1 h. PCR was performed in a 20-μl volume containing 0.5 U of AmpliTaq DNA polymerase (Applied Biosystems), 16.6 mM $(NH_4)_2SO_4$, 67 mM Tris–HCl, 6.7 mM $MgCl_2$, 10 mM 2-mercaptoethanol, 1 mM dNTPs, and 1.5 μM sense and antisense primers, using an ABI 9600 thermal cycler (Applied Biosystems). The amplification protocol included 28–30 cycles of 95 °C for 45 s, 58 °C for 1 min, and 72 °C for 1 min. Primer sequences are shown in Supplemental Table 2. RT-PCR was performed in triplicate for each sample-primer set. Each sample was normalized relative to *polymerase (RNA) II (DNA directed) polypeptide L (POLR2L)*. *POLR2L* is a housekeeping gene that showed relatively stable gene expression in various tissues [29]. The PCR products were semi-quantitatively analyzed with ImageJ software (http://rsb.info.nih.gov/ij/).

RTD-PCR

Intron-origin transcript expression was quantified using TaqMan Universal Master Mix (Applied Biosystems). The samples were amplified using an ABI PRISM 7900HT Sequence Detection System (Applied Biosystems). Using the standard curve methods, quantitative PCR was performed in duplicate for each sample-primer set. Each sample was normalized relative to *POLR2L*. The assay IDs used were Hs00185873_m1 for *ACOX2* and Hs00360764_m1 for *POLR2L*. The specific primers and probe sequence of intronic-*ACOX2-1* were 5′-TTCATAAAGTTGTGAGCA-GAGGAAA-3′ (forward), 5′-TGCACCACTTACTGAGCATCTACTC-3′ (reverse), and 5′-ACTTCTTACCTCAGAGCTG-3′ (probe).

Analysis of pathway network

MetaCore™ software (GeneGo Inc., St. Joseph, MI) was used to investigate the molecular pathway networks of non-B, non-C HCC, HBV-HCC and HCV-HCC. All genes up-regulated more than five-fold in all HCC libraries subjected to Enrichment analysis in GO process networks by default settings ($p<0.05$).

Statistical analysis

Kruskal–Wallis tests were used to compare the expression among normal liver, non-cancerous tissues, and HCC tissues. Mann–Whitney *U* tests were also used to evaluate the statistical significance of ACOX2

Please cite this article as: Y. Hodo, et al., Comprehensive gene expression analysis of 5′-end of mRNA identified novel intronic transcripts associated with hepatocellular carcinoma, Genomics (2010), doi:10.1016/j.ygeno.2010.01.004

gene expression levels between two groups. All statistical analyses were performed using R (http://www.r-project.org/).

Acknowledgments

The authors would like to thank Mr. Shungo Deshimaru and Ms. Keiko Harukawa for technical assistance.

Appendix A. Supplementary data

Supplementary data associated with this article can be found, in the online version, at doi:10.1016/j.ygeno.2010.01.004.

References

[1] H.B. El-Serag, K.L. Rudolph, Hepatocellular carcinoma: epidemiology and molecular carcinogenesis, Gastroenterology 132 (2007) 2557–2576.
[2] Y. Yokoi, S. Suzuki, S. Baba, K. Inaba, H. Konno, S. Nakamura, Clinicopathological features of hepatocellular carcinomas (HCCs) arising in patients without chronic viral infection or alcohol abuse: a retrospective study of patients undergoing hepatic resection, J. Gastroenterol. 40 (2005) 274–282.
[3] R.N. Aravalli, C.J. Steer, E.N. Cressman, Molecular mechanisms of hepatocellular carcinoma, Hepatology 48 (2008) 2047–2063.
[4] D.J. Duggan, M. Bittner, Y. Chen, P. Meltzer, J.M. Trent, Expression profiling using cDNA microarrays, Nat. Genet. 21 (1999) 10–14.
[5] V.E. Velculescu, L. Zhang, B. Vogelstein, K.W. Kinzler, Serial analysis of gene expression, Science 270 (1995) 484–487.
[6] T. Yamashita, S. Hashimoto, S. Kaneko, S. Nagai, N. Toyoda, T. Suzuki, K. Kobayashi, K. Matsushima, Comprehensive gene expression profile of a normal human liver, Biochem. Biophys. Res. Commun. 269 (2000) 110–116.
[7] S. Hashimoto, S. Nagai, J. Sese, T. Suzuki, A. Obata, T. Sato, N. Toyoda, H.Y. Dong, M. Kurachi, T. Nagahata, K. Shizuno, S. Morishita, K. Matsushima, Gene expression profile in human leukocytes, Blood 101 (2003) 3509–3513.
[8] H. Okabe, S. Satoh, T. Kato, O. Kitahara, R. Yanagawa, Y. Yamaoka, T. Tsunoda, Y. Furukawa, Y. Nakamura, Genome-wide analysis of gene expression in human hepatocellular carcinomas using cDNA microarray: identification of genes involved in viral carcinogenesis and tumor progression, Cancer. Res. 61 (2001) 2129–2137.
[9] Y. Shirota, S. Kaneko, M. Honda, H.F. Kawai, K. Kobayashi, Identification of differentially expressed genes in hepatocellular carcinoma with cDNA microarrays, Hepatology 33 (2001) 832–840.
[10] T. Yamashita, M. Honda, S. Kaneko, Application of serial analysis of gene expression in cancer research, Curr. Pharm. Biotechnol. 9 (2008) 375–382.
[11] Y. Suzuki, H. Taira, T. Tsunoda, J. Mizushima-Sugano, J. Sese, H. Hata, T. Ota, T. Isogai, T. Tanaka, S. Morishita, K. Okubo, Y. Sakaki, Y. Nakamura, A. Suyama, S. Sugano, Diverse transcriptional initiation revealed by fine, large-scale mapping of mRNA start sites, EMBO Rep. 2 (2001) 388–393.
[12] K. Kimura, A. Wakamatsu, Y. Suzuki, T. Ota, T. Nishikawa, R. Yamashita, J. Yamamoto, M. Sekine, K. Tsuritani, H. Wakaguri, S. Ishii, T. Sugiyama, K. Saito, Y. Isono, R. Irie, N. Kushida, T. Yoneyama, R. Otsuka, K. Kanda, T. Yokoi, H. Kondo, M. Wagatsuma, K. Murakawa, S. Ishida, T. Ishibashi, A. Takahashi-Fujii, T. Tanase, K. Nagai, H. Kikuchi, K. Nakai, T. Isogai, S. Sugano, Diversification of transcriptional modulation: large-scale identification and characterization of putative alternative promoters of human genes, Genome. Res. 16 (2006) 55–65.
[13] T. Shiraki, S. Kondo, S. Katayama, K. Waki, T. Kasukawa, H. Kawaji, R. Kodzius, A. Watahiki, M. Nakamura, T. Arakawa, S. Fukuda, D. Sasaki, A. Podhajska, M. Harbers, J. Kawai, P. Carninci, Y. Hayashizaki, Cap analysis gene expression for high-throughput analysis of transcriptional starting point and identification of promoter usage, Proc. Natl. Acad. Sci. U. S. A. 100 (2003) 15776–15781.
[14] S. Hashimoto, Y. Suzuki, Y. Kasai, K. Morohoshi, T. Yamada, J. Sese, S. Morishita, S. Sugano, K. Matsushima, 5′-end SAGE for the analysis of transcriptional start sites, Nat. Biotechnol. 22 (2004) 1146–1149.
[15] T. Yamashita, S. Kaneko, S. Hashimoto, T. Sato, S. Nagai, N. Toyoda, T. Suzuki, K. Kobayashi, K. Matsushima, Serial analysis of gene expression in chronic hepatitis C and hepatocellular carcinoma, Biochem. Biophys. Res. Commun. 282 (2001) 647–654.
[16] T. Yamashita, M. Honda, H. Takatori, R. Nishino, H. Minato, H. Takamura, T. Ohta, S. Kaneko, Activation of lipogenic pathway correlates with cell proliferation and poor prognosis in hepatocellular carcinoma, J. Hepatol. 50 (2009) 100–110.
[17] J.S. Mattick, Introns: evolution and function, Curr. Opin. Genet. Dev. 4 (1994) 823–831.
[18] J.S. Mattick, I.V. Makunin, Non-coding RNA, Hum. Mol. Genet. 15 (Spec No 1) (2006) R17–29.
[19] R. Louro, A.S. Smirnova, S. Verjovski-Almeida, Long intronic noncoding RNA transcription: expression noise or expression choice? Genomics 93 (2009) 291–298.
[20] S. Yu, S. Rao, J.K. Reddy, Peroxisome proliferator-activated receptors, fatty acid oxidation, steatohepatitis and hepatocarcinogenesis, Curr. Mol. Med. 3 (2003) 561–572.
[21] N. Kondoh, T. Wakatsuki, A. Ryo, A. Hada, T. Aihara, S. Horiuchi, N. Goseki, O. Matsubara, K. Takenaka, M. Shichita, K. Tanaka, M. Shuda, M. Yamamoto, Identification and characterization of genes associated with human hepatocellular carcinogenesis, Cancer. Res. 59 (1999) 4990–4996.
[22] Y. Kobayashi, T. Higashi, K. Nouso, H. Nakatsukasa, M. Ishizaki, T. Kaneyoshi, N. Toshikuni, K. Kariyama, E. Nakayama, T. Tsuji, Expression of MAGE, GAGE and BAGE genes in human liver diseases: utility as molecular markers for hepatocellular carcinoma, J. Hepatol. 32 (2000) 612–617.
[23] A.H. Minn, M. Kayton, D. Lorang, S.C. Hoffmann, D.M. Harlan, S.K. Libutti, A. Shalev, Insulinomas and expression of an insulin splice variant, Lancet 363 (2004) 363–367.
[24] H. Stier, H.D. Fahimi, P.P. Van Veldhoven, G.P. Mannaerts, A. Volkl, E. Baumgart, Maturation of peroxisomes in differentiating human hepatoblastoma cells (HepG2): possible involvement of the peroxisome proliferator-activated receptor alpha (PPAR alpha), Differentiation 64 (1998) 55–66.
[25] S. Zha, S. Ferdinandusse, J.L. Hicks, S. Denis, T.A. Dunn, R.J. Wanders, J. Luo, A.M. De Marzo, W.B. Isaacs, Peroxisomal branched chain fatty acid beta-oxidation pathway is upregulated in prostate cancer, Prostate 63 (2005) 316–323.
[26] K. Tokuoka, Y. Nakajima, K. Hirotsu, I. Miyahara, Y. Nishina, K. Shiga, H. Tamaoki, C. Setoyama, H. Tojo, R. Miura, Three-dimensional structure of rat-liver acyl-CoA oxidase in complex with a fatty acid: insights into substrate-recognition and reactivity toward molecular oxygen, J. Biochem. 139 (2006) 789–795.
[27] K. Meyer, Y. Jia, W.Q. Cao, P. Kashireddy, M.S. Rao, Expression of peroxisome proliferator-activated receptor alpha, and PPARalpha regulated genes in spontaneously developed hepatocellular carcinomas in fatty acyl-CoA oxidase null mice, Int. J. Oncol. 21 (2002) 1175–1180.
[28] N. Tanaka, K. Moriya, K. Kiyosawa, K. Koike, F.J. Gonzalez, T. Aoyama, PPARalpha activation is essential for HCV core protein-induced hepatic steatosis and hepatocellular carcinoma in mice, J. Clin. Invest. 118 (2008) 683–694.
[29] C. Rubie, K. Kempf, J. Hans, T. Su, B. Tilton, T. Georg, B. Brittner, B. Ludwig, M. Schilling, Housekeeping gene variability in normal and cancerous colorectal, pancreatic, esophageal, gastric and hepatic tissues, Mol. Cell. Probes. 19 (2005) 101–109.

Please cite this article as: Y. Hodo, et al., Comprehensive gene expression analysis of 5′-end of mRNA identified novel intronic transcripts associated with hepatocellular carcinoma, Genomics (2010), doi:10.1016/j.ygeno.2010.01.004

Diabetes Publish Ahead of Print, published online December 3, 2009

CD14$^+$ monocytes are vulnerable and functionally impaired under ER stress in patients with type 2 diabetes

A short running title: Diabetic monocyte is attenuated under ER stress

Takuya Komura [1], Yoshio Sakai [1], Masao Honda [1],
Toshinari Takamura [1], Kouji Matsushima [2], Shuichi Kaneko [1]

[1] Disease Control and Homeostasis, Kanazawa University, Graduate School of Medical Science.
[2] Department of Molecular Prevent Medicine, School of Medicine, The University of Tokyo.

Corresponding author:
Shuichi Kaneko, M.D., Ph.D.
Email: skaneko@m-kanazawa.jp

Additional information for this article can be found in an online appendix at
http://diabetes.diabetesjournals.org

Submitted 13 May 2009 and accepted 16 November 2009.

Objective—While patients with diabetes suffer from increased infections and a higher incidence of cancer due to impaired immune function, details on diabetes-induced decrease in immunity are lacking. We assessed how immune-mediating peripheral blood mononuclear cells (PBMCs) are affected in diabetes.

Research designs and methods—We obtained PBMCs from 33 patients with type 2 diabetes and 28 healthy volunteers, and investigated their susceptibility to apoptosis and functional alteration.

Results—In a subpopulation of PBMCs, monocytes derived from patients with diabetes were more susceptible to apoptosis than monocytes from healthy volunteers. Monocytes from patients with diabetes had decreased phagocytotic activity and were less responsive to Toll-like receptor (TLR) ligands, although the expression of TLRs did not differ significantly between the two groups. Furthermore, monocytes from patients with diabetes had a distinctly different gene expression profile compared to monocytes from normal volunteers as assessed with DNA microarray analysis. Specifically, quantitative real-time detection PCR measurements showed an elevated expression of the markers of endoplasmic reticulum (ER) stress in diabetic monocytes, and electron microscopic examination of monocytes revealed morphological alterations in the ER of cells derived from patients with diabetes. Consistently, the ER stress inducer tunicamycin increased apoptosis of otherwise healthy monocytes and attenuated the pro-inflammatory responses to TLR ligands.

Conclusions—These data suggest that monocytes comprise a substantially impaired subpopulation of PBMCs in patients with diabetes and that ER stress is involved in these pathological changes mechanistically. This implies that the affected monocytes should be investigated further to better understand diabetic immunity.

Type 2 diabetes is the most frequent metabolic disease and the leading cause of human morbidity and mortality (1, 2). Based on epidemiological data, patients with diabetes are immunocompromised and have an increased incidence of infections in the respiratory tract, urinary tract, and skin (3–5). The high incidence of colorectal, breast, and pancreatic malignancies in patients with diabetes is also considered to be a consequence of diabetes-associated defects in immune function (6, 7).

Although studies on immune cells and circulating cytokines have shed some light on this diabetic immunological phenomenon, conflicting results have been reported and do not adequately explain the perturbed immune function in patients with diabetes. Controversial results concerning the phagocytotic activity of polymorphonuclear neutrophils and monocytes are in part due to differences in the patients themselves, insufficient numbers in the study populations, or inconsistencies in the collection of the cell populations under investigation (8–11). Therefore, further studies are needed to explain the decreased immune function of patients with diabetes.

We previously investigated the gene expression signatures of peripheral blood mononuclear cells (PBMCs) in patients with diabetes and observed transcriptional expression features that were distinct from those of healthy volunteers (12). Apoptosis-related genes were up-regulated in the PBMCs of patients with diabetes. Based on this result, we investigated apoptotic activity and immunological function in PBMCs from patients with type 2 diabetes.

We observed that the $CD14^+$ monocyte fraction was the most affected subpopulation of PBMCs from these patients; these cells were especially vulnerable to apoptosis compared to other cell subpopulations. We also found that $CD14^+$ monocytes demonstrated attenuated phagocytotic activity and deficient Toll-like receptor (TLR) signaling, both of which are important for innate immunity (13, 14). Transcriptional analysis and electron microscopic examination of monocytes from patients with diabetes showed evidence of endoplasmic reticulum (ER) stress, which may underlie the functional defects in these cells. Collectively, the data presented herein show that $CD14^+$ monocytes are a vulnerable cell population under ER stress in these patients that could contribute to decreases in immune function in diabetes.

RESERCH DESIGN AND METHODS

Patients: Thirty-three patients with type 2 diabetes (male/female, 15/18; age, 62.0 ± 8.6 years; HbA_{1c}, 9.2 ± 2.0%) and 28 healthy volunteers (male/female, 15/13; age, 58.2 ± 10.2 years; HbA_{1c}, 5.4 ± 0.7%) were enrolled consecutively for the apoptosis assay (Table 1). The groups were not significantly different in terms of their clinical parameters, except for the fasting plasma glucose (FPG) and HbA_{1c} levels. The patients with diabetes (n = 16) from whom adequate numbers of monocytes were obtained were enrolled for additional experiments along with 17 other patients with diabetes (male/female, 8/9; age, 60.5 ± 7.2 years; HbA_{1c} 8.8 ± 1.8) whose clinical profiles fit the diabetic profile (Table 1). Informed consent for this study was obtained from all subjects. The experimental protocol was carried out in accordance with the Declaration of Helsinki.

Isolation of subpopulations of PBMCs and flow cytometric analysis: PBMCs were freshly isolated from heparinized venous blood using Ficoll–Hypaque (Sigma–Aldrich, St. Louis, MO) as previously described (12). $CD4^+$ T cell and $CD14^+$ monocyte subpopulations were isolated using a magnetic cell sorting

system in accordance with the manufacturer's protocol (Miltenyi Biotec, Bergisch Gladbach, Germany). Isolated cells were purified by > 90 % as measured by flow cytometric analysis using FACSCalibur™ flow cytometer (BD Biosciences, San Jose, CA). To assess the expression of TLRs on monocytes, PBMCs were incubated with phosphatidylethanolamine (PE)-labeled anti-TLR2, TLR3, or TLR4 (eBioscience, San Diego, CA) and fluorescein isothiocyanate (FITC)-labeled anti-CD14 antibodies (BD Biosciences) and analyzed by flow cytometry. Data were analyzed using CELLQuest™ Software (BD Biosciences).

Quantitative real-time detection PCR (RTD-PCR): RTD-PCR was performed as previously described (15). Briefly, total RNA obtained from cells using a MicroRNA isolation kit (Stratagene, La Jolla, CA) was reverse-transcribed using 1 μg oligo (dT) primer and Super Script II Reverse transcriptase (Invitrogen, Carlsbad, CA). The relative quantities of mRNA expression were analyzed by RTD-PCR using ABI PRISM 7900 HT Sequence Detection System (Applied Biosystems, Foster City, CA). All primer pairs and probes were obtained from the TaqMan assay reagents library. Expression levels of genes were calculated with the $2^{-\Delta\Delta Ct}$ method using either β-actin or GAPDH as internal control genes.

Apoptotic cell detection assay: Freshly isolated PBMCs were incubated with AIM-V (Invitrogen) serum-free culture media containing 5 or 30 mM glucose at 37°C with 5% CO_2 for up to 24 h. The cells were incubated with FITC-labeled anti-CD4, CD14, or CD56 antibodies (BD Biosciences) and with PE-labeled Annexin-V and 7-amino-actinomycin D (7-AAD) (BD Biosciences) in PBS containing 2% BSA (Sigma–Aldrich). Apoptotic cells were determined by flow cytometry as the fraction of cells labeled with Annexin-V that were 7-AAD negative. At least 10,000 cells per sample were analyzed.

Phagocytosis assay: Phagocytotic activity was assessed using Phagotest Kit (Orpegen Pharma, Heidelberg, Germany) and FITC-labeled opsonized *E. coli* in accordance with manufacturer's protocol. Briefly, heparinized whole blood obtained from the 33 patients with diabetes and 28 healthy volunteers was incubated with FITC-labeled *E. coli* for 10 min at 37°C. After removing the erythrocytes, the remaining cells were incubated with propidium iodide to detect viable leukocytes by flow cytometry. Monocyte populations were assessed based on cellular granularity and size as side scatter and forward scatter, respectively, and FITC-positive cells were assessed as monocytes with phagocytosed FITC-labeled *E. coli*.

TLR ligand stimuli and expression of pro-inflammatory cytokine genes: Peptidoglycan (PGN) (1 μg/ml) from *Streptomyces sp.* (Sigma–Aldrich), Poly (I:C) (5 μg/ml) (Sigma–Aldrich), and Lipopolysaccharide (LPS) (2 μg/ml) from *E. coli* (Sigma–Aldrich), which are TLR2, TLR3, and TLR4 ligands, respectively, were added to monocytes (3×10^5cells) freshly isolated from the 33 patients and 28 healthy volunteers in AIM-V media. Before and 3 h after incubation, the expression of tumor necrosis factor-α (TNF-α) and interleukin-1β (IL-1β) was analyzed by RTD-PCR.

Analysis of gene expression by DNA microarray: Total RNA was obtained from $CD14^+$ monocytes using MicroRNA isolation kit (Stratagene, La Jolla, CA), and the mRNA was amplified twice using the Amino-allyl MessageAmp aRNA Kit (Ambion, Austin, TX). The reference RNA sample was isolated from $CD14^+$ monocytes from a 30-year-old healthy male volunteer and amplified in the same manner. Amplified mRNA was labeled with Cyanine (Cy) 5 or Cy3 (Amersham, Buckinghamshire, UK).

Equal amounts of the amplified mRNAs were hybridized to an oligo-DNA chip (AceGene®Human Oligo Chip 30K; Hitachi Software Engineering Co., Yokohama, Japan) overnight and washed prior to image scanning.

The fluorescence intensity of each spot on the oligo-DNA chip was obtained using cDNA Microarray Scan Array G (PerkinElmer, Wellesley, MA). The obtained images were quantified using DNAsis array v2.6 software (Hitachi Software Engineering Co.). For normalization, the intensity of each spot with oligo DNA was subtracted from that of spots without oligo DNA in the same block. The spot was validated when the intensity was within the intensity plus or minus a 2-fold range of standard deviation within each block. By calibrating the median as the base value, the intensities of all spots were adjusted for normalization between Cy5 and Cy3. Hierarchical clustering of gene expression was calibrated using the method described above using BRB Array Tools (http://linus.nci.nih.gov/BRB-ArrayTools.html). The non-filtered data were log-transformed and applied to the average linkage clustering with centered correlation. For the functional analysis of the 813 upregulated genes, we used GenMAPP (http://www.genmapp.org), a computer program designed for viewing and analyzing genome-scale data on MAPPs representing biological pathways and any other groups of genes.

Electron microscopy: Monocytes obtained from 3 healthy volunteers and 3 patients with diabetes were fixed with 2.5% glutaraldehyde, and then post-fixed in 1% (v/v) cacodylate-buffered osmium tetroxide. Samples were dehydrated in a graded series of ethanol, transferred to propylene oxide, and embedded in Epon-Araldite. Ultrathin sections were obtained and observed under a Hitachi H-7500 electron microscope (Hitachi High-Technologies Co., Hitachinaka, Japan).

Caspase-3 assay and enzyme-linked immunosorbent assay (ELISA) of cytokines: Monocytes from a healthy volunteer were harvested and treated with tunicamycin (1 or 5 μg/ml) in AIM-V media. Every 3 h up to 12 h after tunicamycin treatment, we assessed apoptosis by flow cytometry as described above. After 12 h of incubation, the expression levels of BCL-2, C/EBP homologous protein (CHOP) and (immunoglobulin heavy chain binding protein) BiP were assessed by RTD-PCR. The DEVD-cleaving activity of active caspase-3 was measured using labeled Asp-Glu-Val-Asp-p-nitroanilide (DEVD-pNA) as the substrate and the Caspase-3 Colorimetric Assay Kit (Promega, Madison, WI) in accordance with manufacturer's protocol. The *p*NA light emission was quantified using a microtiter plate reader at a wavelength of 405 nm. In addition, we measured the production of pro-inflammatory cytokines by RTD-PCR 6 h after treatment of monocytes (3×10^5 cells) with tunicamycin (1 or 5 μg/ml) or the TLR ligands PGN (1 μg/ml), Poly (I:C) (5 μg/ml), and LPS (2 μg/ml). The concentrations of TNF-α, IL-1β, and IL-6 in the culture supernatants were measured using ELISA kit (eBioscience).

Statistical analysis: Data are expressed as means ± SEM. The Mann–Whitney *U* test was applied to assess the significant differences between the two groups. Statistical significance was determined as * $P < 0.05$, ** $P < 0.01$, *** $P < 0.001$.

RESULTS

Increased apoptosis of $CD14^+$ monocytes from patients with diabetes: We first assessed the frequency of apoptosis in the PBMC fractions from 33 patients with diabetes and 28 non-diabetic, healthy volunteers. Apoptosis of the isolated cells was assessed after 3 h incubation in AIM-V

serum-free media containing 5 mM glucose (physiological concentration in blood). As shown in Fig. 1*A*, a significant difference in the frequency of apoptosis was observed in the PBMCs isolated from patients with diabetes and healthy volunteers. Adding serum to AIM-V serum-free media did not affect the difference in apoptosis (data not shown). The numbers of whole PBMCs, $CD4^+$, $CD14^+$, and $CD56^+$ cells were similar in both diabetic and healthy subjects (data not shown). $CD14^+$ monocytes were observed to be the major contributor to the increased apoptosis measured in the PBMCs. In contrast, apoptosis of $CD4^+$ T cells and $CD56^+$ NK cells were not significantly different between the two groups (Fig. 1*A*). When the incubation period in culture media with or without serum was extended to 24 h, about 20% of the $CD56^+$ NK cells of both patients with diabetes and healthy volunteers were induced to undergo apoptosis. When incubation period was extended to 5 days, about 5% of $CD4^+$ T cells of both patients with diabetes and healthy volunteers were induced to undergo apoptosis; there was no significant difference in cell viability of $CD56^+$ NK cells and $CD4^+$ T cells between the two groups (data not shown). BCL-2 expression of $CD4^+$ T cells was not different between the two groups (data not shown). Apoptosis of PBMC subpopulations incubated in culture media containing 30 mM glucose was not different from cells incubated in 5 mM glucose-containing media (data not shown). Moreover, the susceptibility of PBMCs from patients with diabetes to apoptosis was not related to clinical features such as vascular complications, insulin treatment, and FPG concentrations (data not shown).

However, among the 33 patients with diabetes, the frequency of apoptotic $CD14^+$ monocytes from those with poor glycemic control ($HbA_{1c} \geq 9.0$) was elevated compared to patients with fair glycemic control ($HbA_{1c} < 9.0$) (Fig. 1*B*). Furthermore, after 3 h incubation, the increased ratio of the expression of the anti-apoptotic gene, BCL-2, was substantially lower in monocytes from the 15 patients with $HbA_{1c} \geq 9.0$ compared to the 18 patients having $HbA_{1c} < 9.0$, as assessed by RTD-PCR (Fig. 1*C*). These data suggest that the monocytes of patients with diabetes are susceptible to apoptosis, especially under conditions of poor glycemic control.

Attenuated function of monocytes from patients with diabetes: To determine if functional alterations exist in monocytes isolated from the 33 patients with diabetes, we cocultured the monocytes with FITC-labeled *E. coli* and counted the number of fluorescent monocytes indigeting the labeled *E. coli* by flow cytometry. The ratio of monocytes that phagocytosed *E. coli* to all monocytes in patients with diabetes was higher than in the healthy volunteers (Fig. 2*A* and *B*). No significant correlation was observed between the ratio of phagocytosed *E. coli* and HbA_{1c} levels among the patients (data not shown).

Next, we assessed the responsiveness of monocytes to external pathogenic stimuli *in vitro*. Monocytes typically express pattern-recognition molecules such as the TLRs that are important for innate immunity against various pathogens (13, 14). The expression levels of TLR2, TLR3, and TLR4 were not significantly different between monocytes from patients with diabetes and those from healthy volunteers, as assessed by RTD-PCR (Fig. 3*A*) and flow cytometry (data not shown). We also found that transcriptional expression of TLR signal molecules (MyD88, IRAK1, and TRAF6 for TLR2 and TLR4 signaling and TRIF for TLR3 signaling) was not altered in diabetic monocytes compared to non-diabetic monocytes (data not shown). Next, we exposed the monocytes from the patients with diabetes and healthy volunteers to the TLR ligands, PGN (a TLR2 ligand),

Poly (I:C) (a TLR3 ligand), and LPS (a TLR4 ligand) and measured the expression of the pro-inflammatory cytokine genes, TNF-α and IL-1β. After incubation, the expression of the cytokines was not significantly different between the groups (Fig. 3*B*), but the responsiveness to PGN, Poly (I:C), and LPS was significantly attenuated in monocytes from patients with diabetes compared to those from healthy volunteers as assessed by RTD-PCR (Fig. 3*C* and *D*). These results demonstrate that the monocytes of patients with diabetes are functionally impaired, which implies that they could contribute to immune deficiency in diabetes.

ER stress is a molecular feature of impaired monocytes: To elucidate the molecular features of the diabetic monocytes that were distinctly susceptible to apoptosis, DNA microarray analysis was performed on $CD14^+$ cells isolated from five randomly selected patients with diabetes and five healthy volunteers. These subjects demonstrated clinical features near the median of all study subjects. Unsupervised hierarchical clustering analysis was performed to assess the gene expression profiles of monocytes obtained from patients with diabetes and healthy volunteers; 17,184 filtered genes were evaluated after excluding genes that were not expressed or those with low expression levels that prevented their analysis in 50 % of the cases. As shown in Fig. 4*A*, two completely discernible clusters formed between the patients with diabetes and the healthy volunteers.

We identified 813 genes that were up-regulated in the monocytes from patients with diabetes compared to those of healthy volunteers ($P < 0.05$, student's t test). Analysis of the biological processes concerning these genes was performed using GenMAPP. The identified genes were shown to be involved in posttranslational protein modification systems occurring in the Golgi-apparatus or were involved in ER stress (Table 2 and Supplemental Table 1 which can be found in an online appendix at http://diabetes.diabetesjournals.org). The elevated expression of genes related to ER stress, such as CHOP and BiP, was confirmed using RTD-PCR; the expression of these genes was significantly higher in the monocytes from the 33 patients with diabetes than in those from the 28 healthy volunteers (Fig. 4*B*). In contrast, no significant difference in the expression of these genes was observed in $CD4^+$ T cells from patients with diabetes and healthy volunteers (Fig. 4*C*).

Electron microscopy further confirmed ER stress in the monocytes derived from patients with diabetes. As shown in Fig. 4*D*, morphological alterations of the ER such as corruption of concentric, continuous and regular layer structure and a decreased number of ribosomes on the ER membrane were evident from the electron photomicrographic images.

ER stress-induced apoptosis and attenuation of TLR signaling in human monocytes: The results described above indicated that the monocytes from patients with diabetes have compromised immunological function and that ER stress is a distinct feature in these cells. To determine whether ER stress could be a mechanism underlying the observed increase in apoptosis and decreased responsiveness to TLR ligands, $CD14^+$ cells isolated from a healthy volunteer were treated with the ER stress inducer, tunicamycin (1 μg/ml), in AIM-V media. As shown in Fig. 5*A* and *B* an increased number of apoptotic cells was observed among monocytes treated with tunicamycin compared to untreated monocytes after more than 6 h incubation. Treatment of monocytes with a higher concentration of tunicamycin (5 μg/ml) induced more apoptosis (Fig. 5*A* and *B*), and when monocytes were treated with tunicamycin for 12 h, the activity of the pro-apoptotic protease, caspase-3,

significantly increased (Fig. 5*C*). Treatment with tunicamycin coordinately decreased the expression of BCL-2 (Fig. 5*D*) and increased the expression of the ER stress markers, CHOP and BiP (Fig. 5*E*). These results suggest that ER stress promotes apoptosis of human monocytes.

Next, we investigated how tunicamycin-induced ER stress affected the responsiveness of human monocytes to TLR ligands. Treatment of monocytes with tunicamycin for 6 h did not affect the transcriptional and translational expression of TLR2 and TLR4 (data not shown). As shown in Fig. 6*A–C*, however, the expression of the pro-inflammatory cytokines TNF-α, IL-1β, and IL-6 were down-regulated after stimulation with TLR2 and TLR4 ligands. Furthermore, the production of TNF-α, IL-1β, and IL-6 in media was measured by ELISA and found to decrease after treatment of human monocytes with tunicamycin and after stimulation with TLR2 or TLR4 ligands (Fig. 6*D–F*). However, tunicamycin-induced ER stress did not affect these expression after treatment of monocytes with the TLR3 ligand, Poly (I:C) (data not shown).

DISCUSSION

In the present study, we observed that PBMCs from patients with diabetes were more susceptible to apoptosis compared to PBMCs from healthy volunteers and that $CD14^+$ monocytes comprised the primary PBMC subpopulation undergoing apoptosis. We also found that $CD14^+$ monocytes from patients with diabetes were hypo-responsive to TLR ligands and that they had attenuated phagocytotic activity. Transcriptional analysis and electron microscopy revealed the presence of ER stress in the affected diabetic monocytes. Consistently, monocytes isolated from non-diabetic patients showed a similar increase in apoptosis and a weakened response to TLR ligands, when they were treated with tunicamycin, indicating that ER stress may be a pivotal mechanism underlying the decreased immunological function observed in patients with diabetes.

As innate immune-defense mediators, monocytes are capable of ingesting exogenous pathogens to protect the host from infectious diseases. Previous studies have shown that phagocytosis in diabetic neutrophils and monocytes is attenuated (10, 11). Similarly, in our study population, monocytes from patients with diabetes were less capable of phagocytosing *E. coli* pathogens compared to monocytes derived from healthy volunteers. This novel finding might explain, at least in part, the decrease in immune function characteristic of patients with diabetes (16). Nevertheless, the detailed mechanisms underlying diabetes-induced decreases in phagocytotic activity remain unclear, since simple high glucose concentration did neither affect the phagocytotic activity and TLR expression, nor induce ER stress in non-diabetic monocytes *in vitro* (data not shown).

The TLRs are pattern recognition receptors that are important for recognizing pathogens, inducing pro-inflammatory responses, and preventing the host from acquiring infectious diseases (17–20). The expression of TLR2, TLR3, and TLR4 in $CD14^+$ monocytes was similar between patients with diabetes and healthy volunteers. The administration of a high dose of insulin downregulates TLRs expression (21). Transformed monocyte-lineage blastoma cells showed increased TLR expression under hyperglycemic conditions in vitro (22). Type 2 diabetes is characterized as a state of inadequately controlled glycemia associated with hyperinsulinemia due to peripheral insulin resistance (1). Taken together, the TLRs expression may be affected by hyperglycemia and hyperinsulinemia in a complex manner. In contrast to the previous finding that monocytes from patients with diabetes were hypersensitive to the TLR

ligand, LPS (23, 24), we observed that the TNF-α and IL-1β expression from monocytes derived from patients with type 2 diabetes diminished after exposure to PGN, Poly I:C, and LPS—ligands of the TLR2, TLR3, and TLR4 receptors, respectively. These data suggest that diabetes perturbs signaling downstream of the TLRs. In this study, we collected $CD14^+$ monocytes from PBMCs via enrichment using magnetic beads; this protocol was used to remove T cells, NK cells, B cells, dendritic cells, and basophils from the PBMC mixture. This is in contrast to the methodology used to isolate these cells in many other studies, in which monocytes were obtained as adherent cells in the culture dish or by a rosetting technique (25, 26). $CD14^+$ cells have been shown to be composed of multiple subtypes of activated states; the classical monocyte-isolation methods used in the other studies might unknowingly remove the fraction of monocytes that are susceptible to apoptosis (27). Over half of the $CD14^+$ diabetic monocytes isolated in this study were dead for 12 h culture even in media containing physiological concentration of glucose (data not shown). Our current data showing attenuation of TLR responsiveness to ligands in diabetic monocytes suggests that initial immune responses that are normally triggered by viruses, bacteria, and parasites could be impaired in diabetes, which is consistent with epidemiological data showing a high incidence of infection in patients with diabetes (3–5).

Gene expression and electron microscopic analysis of monocytes derived from patients with diabetes showed active signatures of ER stress; this is important because ER is an organelle essential for the proper folding and glycosylation of proteins after protein synthesis (28). When cells are under ER stress, protein kinase R-like ER kinase, inositol requiring enzyme 1, and activating transcription factor 6 are activated and function in the adaptation to stress, proper folding of proteins, and removal of harmful unfolded proteins, respectively (29, 30). However, prolonged ER stress leads to apoptotic cell death, which is mediated by CHOP (31). CHOP is a crucial and specific molecule for ER stress-induced apoptosis and alters the transcription of the BCL-2 gene family members (32). The current study showed that diabetic monocytes had increased levels of ER stress-related apoptotic molecules. Moreover, non-diabetic monocytes treated with tunicamycin, an ER stress inducer, underwent apoptosis in a manner similar to monocytes derived from patients with diabetes. From these data, we conclude that ER stress contributes to the susceptibility of diabetic monocytes to apoptosis.

We also observed that tunicamycin-induced ER stress diminished TLR2 and TLR4 signaling without altering expression of TLRs. Tunicamycin induces ER stress by disturbing N-linked glycosylation (33), and previous reports suggest that perturbations in this glycosylation attenuates TLR2 and TLR4 signaling *in vitro* (34, 35). Hence, these data collectively indicate that ER stress may underlie decreases in TLR2 and TLR4 signaling and affect immune function in patients with diabetes.

TLR3 signaling is different from the other TLR signaling pathway; for example, it is independent of MyD88. TLR2 and TLR4 are expressed on the cell surface, whereas TLR3 is expressed in intracellular compartments such as endosomes (13), and its ligands require internalization before signaling occurs. This suggests that disturbances in TLR3 signaling in diabetic monocytes may be due to reasons other than ER stress. Further investigations are needed to elucidate the detailed mechanisms of attenuated TLR signaling in monocytes from patients with diabetes.

ER stress has been shown to be a mainstay of the diabetic condition. Its pathological importance in diabetes is

especially important in pancreatic β-cells, in which glucose toxicity results in ER stress and insufficient insulin secretion (36–38). The current study suggests that monocytes are yet another population of cells vulnerable to hyperglycemia-induced ER stress and dysfunction. Nevertheless, the mechanisms that render pancreatic β-cells and monocytes vulnerable to ER stress in patients with diabetes remain uncertain.

Diabetes is considered a chronic inflammatory disease. Activated macrophages that produce pro-inflammatory cytokines such as TNF-α, IL-1β and IL-6 are thought to contribute to insulin resistance in muscle and adipose tissues (39, 40). Furthermore, the atherosclerotic complications in patients with diabetes have a basis in inflammation; local inflammatory foci in atherosclerotic lesions are commonly composed of foam cells derived from activated macrophages (41, 42). Further studies are needed to determine whether different subpopulations of monocyte-derived cells, for example, systemically circulating and locally residing inflammatory cells, are susceptible to hyperglycemia-induced ER stress and dysfunction.

In conclusion, our findings show that $CD14^+$ monocytes are susceptible to ER stress-induced alterations in inflammatory signaling and apoptosis, which may play a role in the decreased immune function observed in patients with diabetes. Further investigations are needed to discern the mechanisms of diabetes-induced ER stress and perturbations in inflammatory signaling in $CD14^+$ monocytes.

ACKNOWLEDGMENTS

We would like to thank Dr. Iseki for valuable advice and critical comments on electron microscopic examination about ER of monocytes.

REFERENCES

1. Stumvoll M, Goldstein BJ, van Haeften TW. Type 2 diabetes: principles of pathogenesis and therapy. Lancet 2005;365:1333-1346
2. Zimmet P, Alberti KG, Shaw J. Global and societal implications of the diabetes epidemic. Nature 2001;414:782-787
3. Joshi N, Caputo GM, Weitekamp MR, Karchmer AW. Infections in patients with diabetes mellitus. N Engl J Med 1999;341:1906-1912
4. Shah BR, Hux JE. Quantifying the risk of infectious diseases for people with diabetes. Diabetes Care 2003;26:510-513
5. Finney SJ, Zekveld C, Elia A, Evans TW. Glucose control and mortality in critically ill patients. JAMA 2003;290:2041-2047
6. Dunn, GP, Old LJ, Schreiber RD. The immunobiology of cancer immunosurveillance and immunoediting. Immunity 2004;21:137-148
7. Karin M, Lawrence T, Nizet V. Innate immunity gone awry: linking microbial infections to chronic inflammation and cancer. Cell 2006;124:823-835
8. Delamaire M, Maugendre D, Moreno M, Le Goff MC. Impaired leucocyte functions in diabetic patients. Diabet Med 1997;14:29-34
9. Geerlings SE, Hoepelman AI. Immune dysfunction in patients with diabetes mellitus (DM). *FE*MS Immunol Med Microbiol 1999;26:259-265
10. Katz S, Klein B, Elian I, Fishman P, Djaldetti M. Phagocytotic activity of monocytes from diabetic patients. Diabetes Care 1983;6:479-482
11. Geisler C, Almdal T, Bennedsen J, Rhodes JM, Kølendorf K. Monocyte functions in diabetes mellitus. Acta Pathol Microbiol Immunol Scand 1982;[C]90:33-37
12. Takamura T, Honda M, Sakai Y, Ando H, Shimizu A, Ota T, Sakurai M, Misu H, Kurita S, Matsuzawa-Nagata N, Uchikata M, Nakamura S, Matoba R, Tanino M, Matsubara K, Kaneko S. Gene expression profiles in peripheral blood mononuclear cells reflect the pathophysiology of type 2 diabetes. Biochem Biophys Res Commun 2007;361:379-384
13. Akira S, Uematsu S, Takeuchi O. Pathogen recognition and innate immunity. Cell 2006;124:783-801
14. Pasare C, Medzhitov R. Toll-like receptors: linking innate and adaptive immunity. Microbes Infect2004; 6:1382-1387
15. Tateno M, Honda M, Kawamura T, Honda M, Kaneko S. Expression profiling of peripheral-blood mononuclear cells from patients with chronic hepatitis C undergoing interferon therapy. J Infect Dis 2007;195:255-267
16. Stuart LM, Ezekowitz RA. Phagocytosis and comparative innate immunity: learning on the fly. Nat Rev Immunol 2008;8:131-141
17. Thoma-Uszynski S, Stenger S, Takeuchi O, Ochoa MT, Engele M, Sieling PA, Barnes PF, Rollinghoff M, Bolcskei PL, Wagner M, Akira S, Norgard MV, Belisle JT, Godowski PJ, Bloom BR, Modlin RL. Induction of direct antimicrobial activity through mammalian toll-like receptors. Science 2001;291:1544-1547
18. Barton GM, Medzhitov R. Toll-like receptor signaling pathways. Science 2003;300:1524-1525
19. Sabroe I, Parker LC, Dower SK, Whyte MK. The role of TLR activation in inflammation. J Pathol 2008;214:126-135
20. Iwasaki A, Medzhitov R. Toll-like receptor control of the adaptive immune responses. Nat Immunol 2004;10:987-995

21. Ghanim H, Mohanty P, Deopurkar R, Sia CL, Korzeniewski K, Abuaysheh S, Chaudhuri A, Dandona P. Acute modulation of Toll-like receptors by insulin 2008;31:1827-1831.
22. Dasu MR, Devaraj S, Zhao L, Hwang DH, and Jialal I. High glucose induces toll-like receptor expression in human monocytes: mechanism of activation. Diabetes 2008;57:3090-3098
23. Desfaits AC, Serri O, Renier G. Normalization of plasma lipid peroxides, monocyte adhesion, and tumor necrosis factor-alpha production in NIDDM patients after gliclazide treatment. Dibetes care 1998;21:487-493
24. Ohno Y, Aoki N, Nishimura A. In vitro production of interleukin-1, interleukin-6, and tumor necrosis factor-alpha in insulin-dependent diabetes mellitus. J Clin Endocrinol Metab 1993;77:1072-1077
25. Renier G, Mamputu JC, Serri O. Benefits of gliclazide in the atherosclerotic process: decrease in monocyte adhesion to endothelial cells. Metabolism 2003;52:13-18
26. Serbina NV, Jia T, Hohl TM, Pamer EG Monocyte-mediated defense against microbial pathogens. Anne Rev Immunol 2008;26:421-452
27. Wahl LM, Wahl SM, Smythies LE, Smith PD. Isolation of human monocyte populations. Curr Protoc Immunol 2009;7:Unit 7. 6A
28. Ron D, Walter P. Signal integration in the endoplasmic reticulum unfolded protein response. Nat Rev Mol Cell Biol 2007;8:519-529
29. Xu C, Bailly-Maitre B, Reed JC. Endoplasmic reticulum stress: cell life and death decisions. J Clin Invest 2005;115:2656-2664
30. Bukau B, Weisseman J, Horwich A. Molecular chaperones and protein quality control. Cell 2006;125:443-451
31. Wang XZ, Ron D. Stress-induced phosphorylation and activation of the transcription factor CHOP (GADD153) by p38 MAP kinase. Science 1996;272:1347-1349
32. McCullough KD, Martindale JL, Klotz LO, Aw TY, and Holbrook NJ. Gadd153 sensitizes cells to endplasmic reticulum stress by down-regulating Bcl2 and perturbing the cellular redox state. Mol Cell Biol 2001;21:1249-1259
33. Kataoka H, Yasuda M, Iyori M, Kiura K, Narita M, Nakata T, Shibata K. Roles of N-linked glycans in the recognition of microbial lipopeptides and lipoproteins by TLR2. Cell Microbiol 2006;8:1199-1209
34. Ohnishi T, Muroi M, Tanamoto K. N-linked glycosylations at Asn(26) and Asn(114) of human MD-2 are required for toll-like receptor 4-mediated activation of NF-kappaB by lipopolysaccaharide. J Immunol 2001;167:3354-3359
35. Weber AN, Morse MA, Gay NJ. Four N-linked glycosylation sites in human toll-like receptor 2 cooperate to direct efficient biosynthesis and secretion. J Biol Chem 2004;279:34589-34594
36. Ozcan U, Cao Q, Yilmaz E, Lee AH, Iwakoshi NN, Ozdelen E, Tuncman G, Görgün C, Glimcher LH, Hotamisligil GS. Endoplasmic reticulum stress links obesity, insulin action, and type 2 diabetes. Science 2004;306:457-461
37. Oyadomari S, Takeda K, Takiguchi M, Gotoh T, Matsumoto M, Wada I, Akira S, Araki E, Mori M. Nitric oxide-induced apoptosis in pancreatic beta cells is mediated by the endoplasmic reticulum stress pathway. Proc Natl Acad Sci U S A 2001;98:10845-10850
38. Simon S, Maziyar S, Jerrold MO. Insulin sensitivity: modulation by nutrients and inflammation. J Clin Invest 2008;118:2992-3002

39. Kahn SE, Hull RL, Utzschneider KM. Mechanisms linking obesity to insulin resistance and type 2 diabetes. Nature 2006;444:840-846
40. Wellen KE, Hotamisligil GS. Inflammation, stress and diabetes. J Clin Invest 2005;115:1111-1119
41. Brownlee M. Biochemistry and molecular cell biology of diabetic complications. Nature 2001;414:813-820
42. Liang CP, Han S, Senokuchi T, Tall AR. The macrophage at the crossroads of insulin resistance and atherosclerosis. Circ Res 2007;100:1546-1555

Table 1 Characteristics of the study subjects

	Diabetic patients (n=33)	Healthy volunteers (n=28)	P value
Age (years)	62.0±8.6	58.2±10.2	N.S
Gender (male/female)	15/18	15/13	N.S
Body mass index	23.5±4.2	23.6±4.8	N.S
White blood cell counts (/ml)	4800±1700	5600±1900	N.S
Lymphocytes (%)	23.5±3.5	22.7±2.5	N.S
Monocytes (%)	5.2±1.6	6.1±2.3	N.S
Hemoglobin (g/dl)	14.1±1.3	13.6±1.6	N.S
Total cholesterol (mg/dl)	182±24	180±35	N.S
Triglyceride (mg/dl)	138±37	163±33	N.S
FPG (mg/dl)	185±38	86±7.4	<0.001
HbA_{1c} (%)	9.2±2.0	5.4±0.7	<0.001
Diabetic complications (+/-) *	19/14	N.A	
Insulin treatment (+/-)	10/23	N.A	

Data are expressed as means±SD.
* Diabetic complications: nephropathy, neuropathy, retinopathy, macroangiopathy

Table 2 Biological processes for up-regulated genes in monocytes of diabetic patients

MAPP Name	Z Score	Permute P
Golgi-apparatus	3.383	0.000
Ribosomal Proteins	3.691	0.002
Unfold protein binding	2.471	0.026
Intracellular protein transport	2.310	0.029
Enzyme liked receptor protein signaling pathway	2.175	0.042
Nuclear Receptor	2.316	0.043
Gametogenesis	-1.998	0.049

FIGURE LEGENDS

FIG. 1

Monocytes contributed to the vulnerability of the PBMCs in patients with diabetes. (*A*)PBMCs were obtained from 33 patients with diabetes and 28 healthy volunteers. Isolated PBMCs were harvested in AIM-V serum-free culture media supplemented with 5 mM glucose for 3 hours and incubated with FITC-labeled anti-CD4, CD14, or CD56 antibodies, together with PE-labeled Annexin-V to assess the frequency of apoptotic cells in each subpopulation of PBMCs. Apoptotic cells were identified by double-staining with PE-labeled Annexin-V and 7-AAD by flow cytometry. The frequencies of apoptotic cells determined as the Annexin-V-positive and 7-AAD-negative population are expressed as mean ± SEM with statistical comparisons for both groups. The non-parametric Mann-Whitney *U* test was used to calculate the *P* value. $*P < 0.05$ $***P < 0.01$ $***P < 0.001$. The PBMCs of patients with diabetes were more susceptible to apoptosis than those of healthy volunteers, and $CD14^+$ monocytes were contributors. (*B*) Among the 33 patients with diabetes, those with poor glycemic control reflected as $HbA_{1c} \geq 9.0$ were more susceptible to apoptosis in $CD14^+$ monocytes. Data are expressed as mean ± SEM with a statistical comparison of both groups. $*P < 0.05$. (*C*) Monocytes were isolated from 15 patients with $HbA_{1c} \geq 9.0$ and 18 patients with $HbA_{1c} < 9.0$. The expression of the BCL-2 gene in their monocytes before and after incubation in AIM-V serum-free media was assessed by RTD-PCR. After 3 h incubation, the expression of BCL-2 was not upregulated in the poor glycemic control group ($HbA_{1c} \geq 9.0$), as compared to the fair control group ($HbA_{1c} < 9.0$). Data are expressed as mean ± SEM with statistical comparisons of both groups. $*P < 0.05$.

FIG. 2

Attenuated phagocytosis activity in diabetic monocytes. Whole PBMCs were incubated with FITC-labeled *E. coli* for 10 minutes followed by PI staining and flow cytometric analysis. (*A*) Gated PI-positive populations were viable leukocyte populations (upper panel). The monocyte population was assessed using granularity (SSC) and size (FSC) (middle panel). For the gated cells indicating viable monocytes, FITC-positive cells were assessed as monocytes containing phagocytosed FITC-labeled *E. coli*. (lower panel). (*B*) The frequency of monocytes containing phagocytosed *E. coli* in patients with diabetes was less than that in healthy volunteers. Data are expressed as means ± SEM. $*P < 0.05$.

FIG. 3

Hyporesponsiveness to TLR ligand stimuli by the monocytes of patients with diabetes. (*A*)-(*D*) Isolated $CD14^+$ monocytes from 33 patients with diabetes and 28 healthy volunteers were cultured in AIM-V serum-free media supplemented with each TLR ligand: PGN, Poly (I:C), and LPS. After 3 h incubation, RNA was isolated from the monocytes and the expression levels of the TNF-α and IL-1β genes were analyzed by RTD-PCR. The basal (pre-stimuli) expression of (*A*) TLR2, TLR3, and TLR4 and (*B*) TNF-α and IL-1β did not differ significantly between the two groups. The TLR ligand-induced expression of (*C*) TNF-α and (*D*) IL-1β was downregulated in the monocytes of patients with diabetes. Data are expressed as means ± SEM. $*P < 0.05$, $**P < 0.01$.

FIG. 4

Monocytes of patients with diabetes were under ER stress. (*A*) The gene expression profiles of representative vulnerable $CD14^+$ monocytes obtained from five patients with diabetes and five healthy volunteers were analyzed using a DNA microarray. Unsupervised hierarchical clustering using 17,184 filtered genes produced two clusters that separated the patients with diabetes from the healthy volunteers without exception. (*B*)–(*C*), The gene expression levels of the ER stress markers, such as CHOP and BiP, on $CD14^+$ monocytes and $CD4^+$ T cells obtained from 33 patients with diabetes and 28 healthy volunteers was analyzed using RTD-PCR. (*B*) The expression levels of CHOP and BiP in monocytes of patients with diabetes were significantly upregulated, as compared to the monocytes of healthy volunteers. Data are expressed as means ± SEM. $*P < 0.05$, $**P < 0.01$. (*C*) The expression levels of CHOP and BiP in T cells of patients with diabetes were similar to those of healthy volunteers. Data are expressed as mean ± SEM. (*D*) Monocytes were obtained from three healthy volunteers and three patients with diabetes (Healthy volunteer 1: 64-year-old man, HbA_{1c} 5.7%; Healthy volunteer 2: 66-year-old man, HbA_{1c} 4.9%; Healthy volunteer 3: 68-year-old woman, HbA_{1c} 5.6%; Diabetic patient 1: 56-year-old man, HbA_{1c} 9.1%; Diabetic patient 2: 64-year-old woman, HbA_{1c} 8.2%; Diabetic patient 3: 71-year-old man, HbA_{1c} 10.2%) and examined them using electron microscopy. In the three patients with diabetes, the concentric, continuous, and regular layer structures of the ER were corrupted, with fewer ribosomes on the ER membrane compared to the ER of the healthy volunteer. ER, endoplasmic reticulum; N, nucleus; M, mitochondrion. Scale bars indicate 100 nm.

FIG. 5

ER stress enhanced the susceptibility of human monocytes to apoptosis. (*A*)–(*B*) Human $CD14^+$ monocytes obtained from a healthy volunteer were incubated in AIM-V culture media supplemented with tunicamycin (1 or 5 μg/ml). The frequency of apoptotic cells was analyzed by flow cytometry every 3 h for 12 h. More apoptotic cells were observed among monocytes treated with tunicamycin for more than 6 h incubation, as compared to untreated monocytes. (*A*) Representative scattergram of Annexin-V and 7-AAD for monocytes treated with tunicamycin. The numbers in each quadrant indicate the percentage of apoptotic cells. (*B*) Apoptotic cells were assessed in triplicate for each condition. Data are expressed as means ± SEM. (*C*) Caspse-3 activity in monocytes treated with tunicamycin increased significantly at 12 h incubation. (*D*) The BCL-2 expression in monocytes incubated with tunicamycin for 12 h was down-regulated. (*E*) The expression levels of the ER stress markers CHOP and BiP in monocytes incubated with tunicamycin for 12 h were significantly up-regulated. Data are expressed as means ± SEM of three independent experiments. Open bars, no treatment; shaded bar, treatment with tunicamycin (1 μg/ml); solid bar, treatment with tunicamycin (5 μg/ml). TM, tunicamycin.

FIG. 6

Expression of pro-inflammatory cytokines in response to TLR ligand stimuli decreased in human monocytes treated with tunicamycin. Isolated human $CD14^+$ monocytes were incubated in AIM-V culture media with tunicamycin (1 or 5 μg/ml) and stimulated using TLR ligands, PGN, and LPS for 6 h. *A–C*, RTD-PCR analysis showed that the expression of TNF-α (*A*), IL-1β (*B*),

and IL-6 (*C*) was down-regulated in human CD14$^+$ monocytes treated with tunicamycin, especially at the higher concentration (5 μg/ml). *D–F*, ELISA showed that the production of TNF-α (*D*), IL-1β (*E*), and IL-6 (*F*) in culture media decreased in human monocytes treated with tunicamycin, especially at the higher concentration (5 μg/ml). Data are expressed as means ± SEM of four independent experiments. Open bars, no treatment; shaded bar, treatment with tunicamycin (1 μg/ml); solid bar, treatment with tunicamycin (5 μg/ml). TM, tunicamycin.

Figure 1